Journal of Solid Mechanics Vol. 15, No. 1 (2023) pp. 1-18
DOI: 10.22034/jsm.2020.1895607.1563

Research Paper

The Frequency Response of Intelligent Composite Sandwich Plate Under Biaxial In-Plane Forces

A.A. Ghorbanpour Arani [1], Z. Khoddami Maraghi [2], A. Ghorbanpour Arani [3,4 *]

[1] *School of Mechnical Engineering, College of Engineering, University of Tehran, Tehran, Iran*
[2] *Faculty of Engineering, Mahallat Institute of Higher Education, Mahallat, Iran*
[3] *Institute of Nanoscience and Nanotechnology, University of Kashan, Kashan, Iran*
[4] *Faculty of Mechanical Engineering, University of Kashan, Kashan, Iran*

Received 1 September 2022; accepted 17 November 2022

ABSTRACT

This paper investigates the frequency response of a smart sandwich plate made of magnetic face sheets and reinforced core with nano-fibers. The effective elastic properties of composite core reinforced with carbon nanotube are estimated by the extended rule of Mixture. The orthotropic visco-Pasternak foundation is examined to study orthotropic angle, damping coefficient, normal, and shear modulus. The top and bottom face sheets of the sandwich are magnetic and their vibrations are controlled by a feedback control system and magneto-mechanical couplings. Also, the sandwich plate is subjected to the compression and extension in-plane forces in both x and y directions. Five coupled equations of motion are derived using Hamilton's principle. These equations are solved by the differential quadrature method. The analysis performed by the third-order shear deformation theory (Reddy's theory) shows useful details of the effective parameters such in-plane forces, modulus of elastic foundation, core-to-face sheet thickness ratio and controller effect of velocity feedback gain on the dimensionless frequency of the sandwich plate. The analysis of such structures can be discussed in the military, aerospace and civil industries.

Keywords : Nanocomposite core; Sandwich structures; Feedback control system; Magnetostrictive face sheets.

1 INTRODUCTION

COMPOSITES are made from a combination of several materials to create properties that are desirable for a particular use that cannot be achieved with any single component. Approximately, fibres with approximate high strength and high modulus are used in a matrix material of fibre-reinforced composite [1-6]. Different types of fibers and polymer matrices are utilized in composites to produce a material with high quality. These materials are used in many fields including aerospace industry, shipping industry, bridge building industry etc. Composite materials and

*Corresponding author. Tel.: +98 31 55912450; Fax: +98 31 55912424.
E-mail address: aghorban@kashanu.ac.ir (A.Ghorbanpour Arani)

the sandwich structures have long been the interest of researchers but in recent decades, smart materials have created a breakthrough. Investigation about nonlinear dynamic of functionally graded (FG) laminated composite plates embedded with a patch of Active Constrained Layer Damping (ACLD) treatment was carried out by Panda and Ray [7]. Piezoelectric fiber-reinforced composite (PFRC) material was used for constraining layer of ACLD treatment. Also fibre-reinforced composite material was considered for each layer of the substrate FG laminated composite plate in which the fibres were longitudinally aligned in the plane parallel to the top or bottom surface of the layer. In this research, a finite element model was developed based on the first-order shear deformation (FSDT) theory and the effect of piezoelectric fibre orientation on the damping characteristics of the overall FG plates was investigated. Nonlinear vibration and bending behaviours of a sandwich plate made from carbon nanotube-reinforced composite (CNTRC) face sheets resting on Pasternak foundation were investigated by Wang and Shen [8]. Micromechanical model was used to estimate the material properties of CNTRC face sheets. Their results showed the influences of core-to-face sheet thickness ratio (CFTR), volume fraction of CNT, foundation stiffness, temperature change and in-plane boundary conditions on the large-amplitude vibration and nonlinear bending analysis of the sandwich plates. Lei et al. [9] analysed the free vibration of FG single walled carbon nanotubes (SWCNTs) reinforced nanocomposite plates by employing the element-free kp-Ritz approach. They assumed that the composite has been graded through the thickness direction according to several linear distributions of the volume fraction of carbon nanotubes (CNT). They also discussed about the influences of width-to-thickness ratio, CNT volume fraction, plate aspect ratio and temperature change on vibration characteristics of different types of FG-CNTRC plates. Natarajan et al. [10] developed QUAD-8 shear flexible element to investigate the bending and free flexural vibration behaviour of the sandwich plates with CNT reinforced face sheets based on higher-order structural theory. They considered the in-plane and rotary inertia terms in the formulation and obtained the governing equations using Lagrange's equation. They also examined the influence of the volume fraction of CNT, core-to-face sheet thickness and thickness ratio on the global/local response of different sandwich plates. Malekzadeh et al. [11] investigated the effect of non-ideal boundary conditions and initial stresses due to in-plane loads on the vibration of the laminated plates. They used the Lindstedt–Poincare perturbation technique to solve the problem and obtained the frequencies and mode shapes of the plate with non-ideal boundary condition. They also compared their result with finite element simulation using ANSYS software and showed the influence of different parameters such as coefficients of foundation, in-plane stresses and boundary conditions on the natural frequencies of the plate. The transient response of laminated composite plates with embedded smart material layers was studied by Lee et al. [12] They used a unified plate theory including the classical, first-order, and third-order plate theories. Terfenol-D layers were used to control the plate vibration suppression by a simple velocity feedback control. Their findings showed the effect of material properties, smart layer position, and smart layer thickness on the vibration suppression of plate. Transient response and center displacement in laminated magnetostrictive plates under thermal vibration were obtained by Hong [13] using generalized differential quadrature (GDQ) method. He also used the velocity feedback to control vibration suppression in a three-layer laminated magnetostrictive plate with four simply supported edges. Likewise, an efficient method was used to compute the results including shear deformation effect with a few grid points. A new Inverse Trigonometric Zigzag Theory was proposed for the static analysis of the laminated composite and the sandwich plates by Sahoo and Singh [14]. In this theory, higher order displacement field across the plate thickness satisfied the continuity conditions. Different features of the laminated composite and the sandwich plates were investigated in the present study and compared with different published results available in literature. Ghorbanpour Arani and Khoddami Maraghi [15] investigated the vibration analysis of magnetostrictive plate under an external follower force and a magnetic field. For this purpose, they employed sinusoidal shear deformation theory (SSDT) to model displacement field. Zhang et al. [16] studied the vibration behavior of moderately thick composite skew plates which is reinforced by different distributions of carbon nanotubes (CNTs) and used from the first-order shear deformation theory (FSDT). Kiani [17] presented free vibration analysis of functionally graded (FG) CNT reinforced composite plates embedded with piezoelectric facesheets using FSDT. He utilized the modified rule of mixtures approach to obtain the mechanical properties of FGCNT reinforced composite plate. Also in another work, Selim et al. [18] investigated active vibration control of previous problem using Reddy's higher-order shear deformation theory. Lei et al. [19] considered vibration of thick quadrilateral composite plates resting on Pasternak substrate under different boundary conditions. They used FSDT to derive the equations of motion and solved them by the improved moving least-squares Ritz (IMLS-Ritz) method. Static and natural frequency responses of a rectangular FGCNT reinforced composite plate resting on Winkler-Pasternak substrate were examined by Duc et al. [20]. Based on Hamilton principle, they determined the equations of motion and employed Navier solution to obtain the results. Nonlinear vibration analysis of FGCNT reinforced composite annular plates embedded with piezoelectric layers was carried out by Keleshteri et al. [21]. They observed a significant influence of both distribution and volume fraction of CNTs on nonlinear natural frequencies of this problem. Mohammadimehr et al.

[22] presented bending, buckling and vibration analysis of FGCNT reinforced microcomposite plate under hydro-thermal environments using third-order shear deformation theory (TSDT). They determined the mechanical, moisture and thermal properties according to the generalized rule of mixture and solved the governing equations by differential quadrature method (DQM). Ansari et al. [23] studied nonlinear vibration of annular sandwich plates with a homogeneous core and FGCNT reinforced composite facesheets. Based on von Kármán nonlinear kinematic assumption, they are derived the equations of motion using higher order shear deformation plate theory (HSDT). Also, this problem with similar details was investigated by Shen et al. [24] for thermally postbuckled rectangular sandwich plates. Fazzolari [25] considered the thermoelastic vibration and stability characteristics of FGCNT reinforced composite (CNTRC) plates under thermal load. He obtained the equations of motion using Hamilton's Principle in conjunction with the method of the power series expansion of the displacement components and employed the Ritz method, based on highly stable trigonometric trial functions, as solution technique. Parida and Mohanty [26] presented the large amplitude vibration analysis of a FG plate resting on Pasternak elastic foundation under thermal environment using HSDT. They utilized a direct iterative method as solution method. Sahoo et al. [27] examined free vibration and transient behavior of carbon/epoxy laminated composite curved shallow shell. They discussed about the effects of different geometrical and material parameters on the dynamic responses of this structure.Free vibration of nanocomposite sandwich plate made of two smart magnetostrictive face sheets is a new subject which is done for the first time. The magnetostrictive material (MsM) is one of the substances in control systems because of its dual nature. Stress changes due to external magnetic field have created Magneto-mechanical coupling in these materials and such a property can be used in systems stability.

In this research CFTR is considered large and magnetostrictive face sheets are used in a feedback control system. In this work, the role of bi-directional in-plane forces is studied when the forces are applied on composite core and face sheets separately. Orthotropic visco-Pasternak foundation is examined to study orthotropic angle, damping coefficient besides Young's and shear modulus. The results of this research consider the influence of important parameters on vibration frequency of the sandwich plate that can be useful in various industries.

2 STRUCTURAL DEFINITION

A schematic diagram of a sandwich plate resting on orthotropic viscoelastic foundation is illustrated in Fig. 1 in which geometrical parameters of length *a*, width *b* and thickness $2h_m + h_c$ are also indicated.

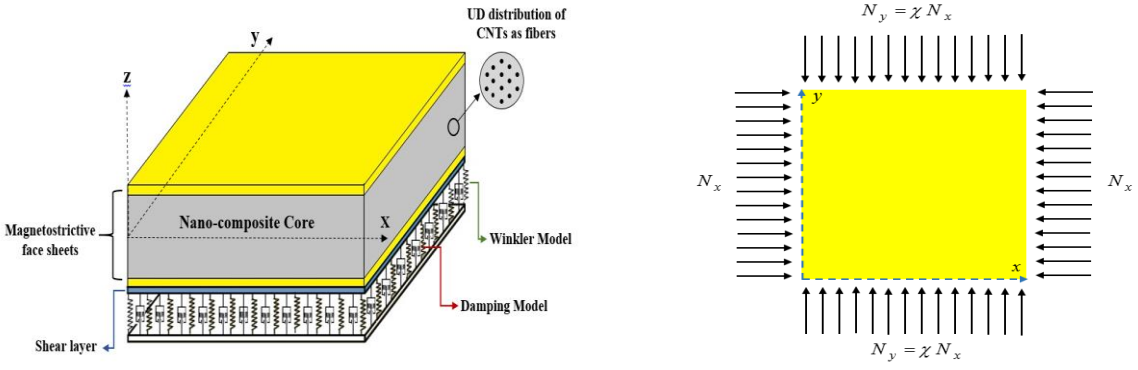

(a) (b)

Fig.1
A schematic diagram of a sandwich plate (a) resting on orthotropic viscoelastic foundation. (b) under biaxial in-plane forces.

As shown in Fig. 1 the sandwich plate is composed of three layers:

a. Central composite core reinforced by CNT,
b. Two face sheets made of MsM.

The strain-displacement relations are separately written for each layer, then forces and moments are obtained. Finally, the total energy including the energy of CNTRC core and magnetostrictive face sheet is obtained. The equation of motions is derived using Hamilton's principle considering viscoelastic foundation and in-plane forces.

3 CONSTITUTIVE EQUATIONS

The following equation is presented for stress-strain relation of isotropic material [28]:

$$\begin{bmatrix}\sigma_{xx}\\ \sigma_{yy}\\ \sigma_{xy}\\ \sigma_{xz}\\ \sigma_{yz}\end{bmatrix}=\begin{bmatrix}\bar{Q}_{11} & \bar{Q}_{12} & 0 & 0 & 0\\ \bar{Q}_{21} & \bar{Q}_{22} & 0 & 0 & 0\\ 0 & 0 & \bar{Q}_{44} & 0 & 0\\ 0 & 0 & 0 & \bar{Q}_{55} & 0\\ 0 & 0 & 0 & 0 & \bar{Q}_{66}\end{bmatrix}\begin{bmatrix}\varepsilon_{xx}\\ \varepsilon_{yy}\\ \varepsilon_{xy}\\ \varepsilon_{xz}\\ \varepsilon_{yz}\end{bmatrix}, \tag{1}$$

where σ_{ij} and ε_{ij} are normal and shear stresses and the stiffness constants are obtained as follows:

$$\bar{Q}_{11}=\bar{Q}_{22}=\frac{E}{(1-\upsilon^2)},\quad \bar{Q}_{12}=\bar{Q}_{13}=\frac{E\upsilon}{(1-\upsilon^2)},\quad \bar{Q}_{44}=\bar{Q}_{55}=\bar{Q}_{66}=\frac{E}{(1+\upsilon)}, \tag{2}$$

In which E and υ are Young modulus and Poisson's ratio respectively. Above equations are valid for CNTRC core and magnetostrictive face sheets ($\bar{C}_{ij}$ instead $\bar{Q}_{ij}$). To this end, the method of obtaining elastic properties of thecomposite core is presented.

3.1 Mechanical properties of CNTRC core h_c

Consider a CNTRC plate with thickness h_c and dimensions $(a\times b)$ .This CNTRC plate is made of two different isotropic materials that called fibers (SWCNT) and polymer matrix (PmPV). The reinforcement fibers are uniformly distributed in length of plate. Extended rule of mixture expresses the material properties of CNTRC plates according to Eq. (3) [9]:

$$\begin{aligned}&E_{11}=\eta_1 V_{CNT}E_{11}^{CNT}+V_m E^m,\\ &\frac{\eta_2}{E_{22}}=\frac{V_{CNT}}{E_{22}^{CNT}}+\frac{V_m}{E^m},\\ &\frac{\eta_3}{G_{12}}=\frac{V_{CNT}}{G_{12}^{CNT}}+\frac{V_m}{G^m},\end{aligned} \tag{3}$$

where E_{11}^{CNT} , E_{22}^{CNT} ,G_{12}^{CNT} , E_m and G_m are the Young's moduli and shear modulus of CNT and isotropic matrix. To account the load transfer between the fibers and matrix such as the surface effect, strain gradient effect, and intermolecular coupled effect on the equivalent material properties of CNTRCs, CNT efficiency parameters η_j (j = 1,2, 3) were introduced by Shen [11] in Eq. (3) [4]. V_{CNT} and V_m are the volume fractions of CNT and matrix. In addition, Poisson's ratio is introduced as follows [9]:

$$\upsilon_{12}=V_{CNT}\upsilon_{12}^{CNT}+V_m\upsilon^m, \tag{4}$$

where υ_{12}^{CNT} is Poisson's ratios of fibers and υ_m is Poisson's ratios of matrix.

The effective thickness of the fibers is a parameter that has been taken into consideration by Lei et al. [9]. They talked about the important role of this parameter in estimating the CNT material properties. Han and Elliott [29] obtained a new value for SWCNTs (10,10) with $h=0.34\,nm$ that presented in Table 1:

Table 1
Material properties of SWCNTs (10,10) with $h = 0.34nm$ [9].

Han and Elliott [24]	E_{11}^{CNT}	E_{22}^{CNT}	G_{12}^{CNT}
SWCNTs (10,10)	600 *GPa*	10 *GPa*	17.2 *GPa*

Also, typical values of effective material properties of SWCNTs(10,10) have been listed in Table 2 [8-10]:

Table 2
Material properties of SWCNTs (10,10) with $h = 0.067nm$ [8-10].

SWCNT (10,10) ($L = 9.26\ nm$, $R = 0.68\ nm$, $h = 0.067\ nm$, $\upsilon_{12}^{CNT} = 0.175$)			
Temperature(K)	E_{11}^{CNT} (TPa)	E_{22}^{CNT} (TPa)	G_{12}^{CNT} (TPa)
300	5.6466	7.0800	1.9445
500	5.5308	6.9348	1.9643
700	5.4744	6.8641	1.9644

Comparing the results of extended rule of mixture and molecular dynamic (MD) simulations, the CNT efficiency parameter is estimated such as Han and Elliott [24] and Griebel and Hamaekers [30] have been reported in Table 3.

Table 3
CNT efficiency parameter for $V_{CNT} = 0.12, 0.17, 0.28$ [29,30].

V_{CNT}	η_1	η_2	η_3
$V_{CNT} = 0.12$	0.137	1.022	0.715
$V_{CNT} = 0.17$	0.142	1.626	1.38
$V_{CNT} = 0.28$	0.141	1.585	1.109
$G_{13} = G_{12}, G_{23} = 1.2G_{12}$			

Also there are other documented results about CNT efficiency parameter that these have been listed in Table 4. [31-32]

Table 4
CNT efficiency parameter for $V_{CNT} = 0.11, 0.14, 0.17$ [31,32].

V_{CNT}	Rule of Mixture	
	η_1	η_2
$V_{CNT} = 0.11$	0.149	0.934
$V_{CNT} = 0.14$	0.150	0.941
$V_{CNT} = 0.17$	0.149	1.381

3.2 Magnetostriction effect

To investigate the effect of the magnetic field on MsM, the magneto-mechanical coupling based on the experimental results appears as follows [33]:

$$\begin{bmatrix} \sigma^m{}_{xx} \\ \sigma^m{}_{yy} \\ \sigma^m{}_{xy} \end{bmatrix} = \begin{bmatrix} \bar{C}_{11} & \bar{C}_{12} & 0 \\ \bar{C}_{21} & \bar{C}_{22} & 0 \\ 0 & 0 & \bar{C}_{44} \end{bmatrix} - \begin{bmatrix} 0 & 0 & e_{31} \\ 0 & 0 & e_{32} \\ 0 & 0 & e_{34} \end{bmatrix} \begin{bmatrix} 0 \\ 0 \\ H_z \end{bmatrix}. \tag{5}$$

Index *m* refers to magnetic stress that summarized by (1) ($\bar{C}_{ij}$ for magnetostrictive face sheets instead $\bar{Q}_{ij}$ for composite core). H_z is the magnetic field intensity and e_{ij} is the magnetostrictive coupling modules which can be expressed as the magnetic field of a coil [12,33-34].

$$H_z = K_c I(x,y,t) = K_c C(t) \frac{\partial w_0(x,y,t)}{\partial t}, \tag{6}$$

where K_c is the coil constant, $I(t)$ is the coil current and $C(t)$ is the control gain. Also, $K_c C(t)$ is defined as velocity feedback gain. In addition, e_{ij} are determined as follows [33]:

$$\begin{aligned} e_{31} &= \tilde{e}_{31}\cos^2\theta + \tilde{e}_{32}\sin^2\theta, \\ e_{32} &= \tilde{e}_{31}\sin^2\theta + \tilde{e}_{32}\cos^2\theta, \\ e_{34} &= (\tilde{e}_{31} - e_{32})\sin\theta\sin\theta, \end{aligned} \tag{7}$$

where θ represents the direction of magnetic anisotropy.

4 THIRD ORDER SHEAR DEFORMATION THEORY (TSDT)

There are some assumptions about TSDT that makes it more accurate than the other theories:

- For a moderately thick plate, shear strains and stresses are not constant through the plate thickness.
- There is not shear correction factor in strain relations.

The displacement field involves a quadratic variation of the transverse shear through the thickness and eliminating transverse shear stresses at the top and bottom surfaces [35-36]. Based on TSDT, the displacement field of plates can be expressed as [36]:

$$\begin{aligned} \tilde{U}(x,y,z,t) &= u_0(x,y,t) + z\,\theta_1(x,y,t) - \frac{4}{3}\frac{z^3}{h^2}\left(\theta_1(x,y,t) + \frac{\partial}{\partial x} w_0(x,y,t)\right), \\ \tilde{V}(x,y,z,t) &= v_0(x,y,t) + z\,\theta_2(x,y,t) - \frac{4}{3}\frac{z^3}{h^2}\left(\theta_2(x,y,t) + \frac{\partial}{\partial y} w_0(x,y,t)\right), \\ \tilde{W}(x,y,z,t) &= w_0(x,y,t), \end{aligned} \tag{8}$$

where $u_0(x,y,t)$, $v_0(x,y,t)$, $w_0(x,y,t)$ are displacement function along (x,y,t) directions and $\theta_1(x,y,t), \theta_2(x,y,t)$ are rotations about x and y axis and t is time. Sandwich plate is considered as a monolithic structure where the displacement of each layers are assumed to be the same according to (8). Eq. (9) presented the linear strain field for TSDT using Hooke's law:

$$\begin{aligned} \varepsilon_{xx} &= \frac{\partial}{\partial x} u_0(x,y,t) + z\,\frac{\partial}{\partial x}\theta_1(x,y,t) - \frac{4}{3}\frac{z^3}{h^2}\left(\frac{\partial}{\partial x}\theta_1(x,y,t) + \frac{\partial^2}{\partial x^2} w_0(x,y,t)\right), \\ \varepsilon_{yy} &= \frac{\partial}{\partial y} v_0(x,y,t) + z\,\frac{\partial}{\partial y}\theta_2(x,y,t) - \frac{4}{3}\frac{z^3}{h^2}\left(\frac{\partial}{\partial y}\theta_2(x,y,t) + \frac{\partial^2}{\partial y^2} w_0(x,y,t)\right), \\ \varepsilon_{zz} &= 0 \\ \varepsilon_{xy} &= \frac{1}{2}\frac{\partial}{\partial x} v_0(x,y,t) + \frac{1}{2} z\,\frac{\partial}{\partial x}\theta_2(x,y,t) - \frac{2}{3}\frac{z^3}{h^2}\left(\frac{\partial}{\partial x}\theta_2(x,y,t) + \frac{\partial^2}{\partial y\,\partial x} w_0(x,y,t)\right), \\ &\quad + \frac{1}{2}\frac{\partial}{\partial y} u_0(x,y,t) + \frac{1}{2} z\,\frac{\partial}{\partial y}\theta_1(x,y,t) - \frac{2}{3}\frac{z^3}{h^2}\left(\frac{\partial}{\partial y}\theta_1(x,y,t) + \frac{\partial^2}{\partial y\,\partial x} w_0(x,y,t)\right), \end{aligned} \tag{9}$$

$$\varepsilon_{xz} = \frac{1}{2}\frac{\partial}{\partial x}w_0(x,y,t)+\frac{1}{2}\theta_1(x,y,t)-2\frac{z^2}{h^2}\left(\theta_1(x,y,t)+\frac{\partial}{\partial x}w_0(x,y,t)\right),$$
$$\varepsilon_{yz} = \frac{1}{2}\frac{\partial}{\partial y}w_0(x,y,t)+\frac{1}{2}\theta_2(x,y,t)-2\frac{z^2}{h^2}\left(\theta_2(x,y,t)+\frac{\partial}{\partial y}w_0(x,y,t)\right). \quad (9)$$

5 ENERGY METHOD IN SANDWICH PLATE

In this section, the energy method is used as a comprehensive method in deriving the equations of motion. Strain energy of the rectangular sandwich plate is calculated as [37]:

$$U = \frac{1}{2}\int_V \left(\sigma_{xx}\varepsilon_{xx}+\sigma_{yy}\varepsilon_{yy}+\tau_{xy}\gamma_{xy}+\tau_{xz}\gamma_{xz}+\tau_{yz}\gamma_{yz}\right)dV,$$
$$U_{sandwich} = U_{Core}+U^{Bottom}_{Face\,sheet}+U^{Top}_{Face\,sheet} = \frac{1}{2}\int_{-\frac{h_c}{2}}^{\frac{h_c}{2}}\int_0^b\int_0^a\left(\sigma_{ij}\varepsilon_{ij}+\tau_{ij}\gamma_{ij}\right)_{Core}dx\,dy\,dz, \quad (10)$$
$$+\frac{1}{2}\int_{-h_m-\frac{h_c}{2}}^{-\frac{h_c}{2}}\int_0^b\int_0^a\left(\sigma_{ij}\varepsilon_{ij}+\tau_{ij}\gamma_{ij}\right)_{Sheet}dx\,dy\,dz+\frac{1}{2}\int_{\frac{h_c}{2}}^{\frac{h_c}{2}+h_m}\int_0^b\int_0^a\left(\sigma_{ij}\varepsilon_{ij}+\tau_{ij}\gamma_{ij}\right)_{Sheet}dx\,dy\,dz.$$

Substituting Eqs. (1), (5) and (9) into Eq. (10), the strain energy of sandwich plate can be obtained. The kinetic energy of sandwich plate can be stated as [38]:

$$K_{Sandwich} = K_{Core}+2K_{Face\,sheet} = \frac{1}{2}(\rho_c h_c+2\rho_m h_m)\left(\int_0^b\int_0^a\left[\left(\frac{\partial\tilde{U}}{\partial t}\right)^2+\left(\frac{\partial\tilde{V}}{\partial t}\right)^2+\left(\frac{\partial\tilde{W}}{\partial t}\right)^2\right]dx\,dy\right). \quad (11)$$

where ρ_c is the density of core and ρ_m is the density of sheets. Substituting (8) into (11), the kinetic energy are obtained.

6 EXTERNAL WORK

6.1 Orthotropic visco-elastic foundation

The Pasternak model has a higher sensitivity than the Winkler model with respect to transverse shear and normal loads [3]. In this paper, the sandwich plate is bonded to the elastic medium by a bottom layer. K_w , g_x , c_d are introduces in visco-elastic Pasternak foundation. The force transmitted on the sandwich plate is from the linear visco-elastic foundation (F) is in the transverse direction. F presented for an arbitrarily oriented orthotropic foundation as follows [39]:

$$F = K_w W - g_x(\cos^2\Theta\frac{\partial^2 W}{\partial x^2}+2\cos\Theta\sin\Theta\frac{\partial^2 W}{\partial x\,\partial y}+\sin^2\Theta\frac{\partial^2 W}{\partial y^2})$$
$$-g_y(\sin^2\Theta\frac{\partial^2 W}{\partial x^2}-2\cos\Theta\sin\Theta\frac{\partial^2 W}{\partial x\,\partial y}+\cos^2\Theta\frac{\partial^2 W}{\partial y^2})-c_d\frac{\partial W}{\partial t}, \quad (12)$$

In which, k_w is Winkler coefficient, K_{gx} and K_{gy} are shear layer coefficients and C_d is damping coefficient.

The angle Θ is the local direction of orthotropic foundation with respect to the global axis of the plate. With the help of the energy method, the work of the elastic foundation can be calculated as:

$$\Sigma = \frac{1}{2}\int_0^b\int_0^a FW\ dxdy\ . \tag{13}$$

6.2 In-plane forces

Since rectangular plates are usually exposed to in-plane forces, the effects of in-plane stresses should be considered in their analysis. Uniform in-plane forces N_x and N_y are applied in x and y directions as shown in Fig. 1(b) and the potential energy due to the in-plane force per unit length in the x and y directions can be written as [40]:

$$U_{In-plane\,force} = \frac{1}{2}\int_0^b\int_0^a\left(N_x\left(\frac{\partial W}{\partial x}\right)^2 + N_y\left(\frac{\partial W}{\partial y}\right)^2\right)dxdy\,. \tag{14}$$

7 HAMILTON'S PRINCIPLE

Hamilton's principle is employed to obtain the equations of motion. The principle can be stated in an analytical form where the first variation form of equations must be zero, as follows [38]:

$$\delta\int_{t_1}^{t_2}\left[U_{Sandwich} - (K_{Sandwich} + \Sigma)\right]dt = 0, \tag{15}$$

where $\delta U_{Sandwich}$, $\delta K_{Sandwich}$ and $\delta\Sigma$ are variation of strain energy, variation of Kinetic energy and variation of external work, respectively. Substituting (10), (11) and (13) and (14) into (15) for TSDT and afterward using dimensionless parameters which introduced in (14):

$$\begin{aligned}
&(\zeta,\eta) = \left(\frac{x}{a},\frac{y}{b}\right),\ (U,V,W) = \left(\frac{u_0}{a},\frac{v_0}{b},\frac{w_0}{h}\right),\ For\ \begin{cases} Core: h_c \\ Face\ sheet: h_m \end{cases}, \gamma = \frac{a}{b}, Q_{ij} = \frac{\bar{Q}_{ij}}{E_m},\quad C_{ij} = \frac{\bar{C}_{ij}}{E_m}\ ,\\
&\in = \frac{E_c}{E_m},\ \delta = \frac{h_c}{h_m},\ (\alpha_m,\beta_m) = \left(\frac{h_m}{a},\frac{h_m}{b}\right),\ (\alpha_c,\beta_c) = \left(\frac{h_c}{a},\frac{h_c}{b}\right), c_{bd} = \frac{c_d\sqrt{\rho_m}}{\sqrt{E_m}},\quad G_{ij} = \frac{e_{ij}\,C(t)K_c}{\sqrt{E_m\rho_m}},\\
&\tau = \frac{t}{a}\sqrt{\frac{E_m}{\rho_m}},\ K_{bw} = \frac{k_w h_m}{E_m},\quad g_{xa} = \frac{g_x}{a.E_m},\ g_{xb} = \frac{g_x}{b.E_m} = \gamma g_{xa},\quad g_{ya} = \frac{g_y}{a.E_m},\quad g_{yb} = \frac{g_y}{b.E_m} = \gamma g_{ya}\ ,\\
&\lambda = \frac{g_{xa}}{g_{ya}},\quad Ibi = \frac{Ii}{h_m^{i+1}}\ (i = 2,4,6),\quad N_{xb} = \frac{N_x}{a.E},\ N_{yb} = \frac{N_y}{b.E}.
\end{aligned} \tag{16}$$

The equations of motion are obtained by setting the coefficient $\delta U, \delta V, \delta W, \delta\theta_1, \delta\theta_2$ equal to zero as follows:

$$\begin{aligned}
&\delta U = \delta U_{core} + \delta U_{Sheet} = (-1/2C_{44}\beta\gamma\frac{d^2U}{d\eta^2} - C_{11}\alpha\frac{d^2U}{d\zeta^2} - 1/2C_{44}\alpha\frac{d^2V}{d\eta d\zeta} - 1/2C_{21}\alpha\frac{d^2V}{d\eta d\zeta}\\
&-1/2C_{12}\alpha\frac{d^2V}{d\eta d\zeta} + \alpha\in\frac{d^2U}{d\tau^2})_{Core} + (-2Q_{11}\alpha_m\frac{d^2U}{d\zeta^2} - Q_{44}\gamma\beta_m\frac{d^2U}{d\eta^2} + G_{31}{\alpha_m}^2\frac{d^2W}{d\tau d\zeta}\\
&-Q_{44}\alpha_m\frac{d^2V}{d\eta d\zeta} - Q_{12}\alpha_m\frac{d^2V}{d\eta d\zeta} - Q_{21}\alpha_m\frac{d^2V}{d\eta d\zeta} + 2\alpha_m\frac{d^2U}{d\tau^2})_{Sheet},
\end{aligned} \tag{17}$$

$$\delta V = \delta V_{Core} + \delta V_{Sheet} = (-1/2\gamma C_{44}\alpha \frac{d^2V}{d\zeta^2} - C_{22}\beta \frac{d^2V}{d\eta^2} - 1/2C_{44}\beta \frac{d^2U}{d\eta d\zeta} - 1/2C_{21}\beta \frac{d^2U}{d\eta d\zeta}$$
$$-1/2C_{12}\beta \frac{d^2U}{d\eta d\zeta} + \frac{\alpha}{\gamma}\epsilon \frac{d^2V}{d\tau^2})_{Core} + (-2Q_{22}\beta_m \frac{d^2V}{d\eta^2} - \frac{Q_{44}\alpha_m}{\gamma}\frac{d^2V}{d\zeta^2} + G_{32}\alpha_m\beta_m \frac{d^2W}{d\tau \mathrm{d}\eta} \quad (18)$$
$$-Q_{44}\beta_m \frac{d^2U}{d\eta d\zeta} - Q_{12}\beta_m \frac{d^2U}{d\eta d\zeta} - Q_{21}\beta_m \frac{d^2U}{d\eta \mathrm{d}\zeta} + 2\frac{\alpha_m}{\gamma}\frac{d^2V}{d\tau^2})_{Sheet},$$

$$\delta W = \delta W_{Core} + \delta W_{Sheet} = (-\frac{4}{15}C_{55}\alpha^2 \frac{d^2W}{d\zeta^2} - \frac{4}{15}C_{66}\beta^2 \frac{d^2W}{d\eta^2} - \frac{2}{315}C_{12}\alpha^2\beta \frac{d^3\theta_2}{d\eta\zeta^2} - \frac{2}{315}C_{21}\alpha^2\beta \frac{d^3\theta_2}{d\eta\zeta^2}$$
$$-\frac{4}{315}C_{44}\beta^2\alpha \frac{d^3\theta_1}{d\eta^2 d\zeta} - \frac{2}{315}C_{21}\beta^2\alpha \frac{d^3\theta_1}{d\eta^2 d\zeta} - \frac{4}{315}C_{22}\beta^3 \frac{d^3\theta_2}{d\eta^3} - \frac{4}{315}C_{11}\alpha^3 \frac{d^3\theta_1}{d\zeta^3} - \frac{4}{315}C_{44}\alpha^2\beta \frac{d^3\theta_2}{d\eta\zeta^2}$$
$$-\frac{4}{15}C_{55}\alpha \frac{d\theta_1}{d\zeta} - \frac{2}{315}C_{12}\beta^2\alpha \frac{d^3\theta_1}{d\eta^2 d\zeta} - 1/2C_{66}\beta \frac{d\theta_2}{d\eta} + \frac{7}{30}C_{66}\alpha \frac{d\theta_2}{d\eta} + \frac{1}{252}C_{22}\beta^4 \frac{d^4W}{d\eta^4}$$
$$+\frac{1}{126}C_{44}\alpha^2\beta^2 \frac{d^4W}{d\eta^2 d\zeta^2} + \frac{1}{252}C_{11}\alpha^4 \frac{d^4W}{d\zeta^4} + \frac{1}{252}C_{12}\alpha^2\beta^2 \frac{d^4W}{d\eta^2 d\zeta^2} + \frac{1}{252}C_{21}\alpha^2\beta^2 \frac{d^4W}{d\eta^2 d\zeta^2}$$
$$+\frac{4}{315}\alpha^3\epsilon \frac{d^3\theta_1}{d\tau^2 d\zeta} - \frac{1}{252}\alpha^4\epsilon \frac{d^4W}{d\tau^2 d\zeta^2} + \frac{4}{315}\alpha^2\beta\epsilon \frac{d^3\theta_2}{d\tau^2 d\eta} - \frac{1}{252}\alpha^2\beta^2\epsilon \frac{d^4W}{d\tau^2 d\eta^2} + \alpha^2\epsilon \frac{d^2W}{d\tau^2})_{Core} +$$
$$(\frac{32}{9}Q_{22}Ib6\beta_m{}^4 \frac{d^4W}{d\eta^4} + \frac{32}{9}Q_{11}Ib6\alpha_m{}^4 \frac{d^4W}{d\zeta^4} + 8Q_{55}Ib2\alpha_m{}^2 \frac{d^2W}{d\zeta^2} - 16Q_{66}Ib4\beta_m{}^2 \frac{d^2W}{d\eta^2}$$
$$+8Q_{66}Ib2\beta_m{}^2 \frac{d^2W}{d\eta^2} - 16Q_{55}Ib4\alpha_m{}^2 \frac{d^2W}{d\zeta^2} - \frac{32}{9}Ib6\alpha_m{}^2\beta_m{}^2 \frac{d^4W}{d\tau^2 d\eta^2} - 8/3Q_{11}Ib4\alpha_m{}^3 \frac{d^3\theta_1}{d\zeta^3}$$
$$+\frac{32}{9}Q_{11}Ib6\alpha_m{}^3 \frac{d^3\theta_1}{d\zeta^3} - 16Q_{55}Ib4\alpha_m \frac{d\theta_1}{d\zeta} + 8Q_{55}Ib2\alpha_m \frac{d\theta_1}{d\zeta} - 8/3Q_{22}Ib4\beta_m{}^3 \frac{d^3\theta_2}{d\eta^3}$$
$$+\frac{32}{9}Q_{22}Ib6\beta_m{}^3 \frac{d^3\theta_2}{d\eta^3} + 8/3Ib4\alpha_m{}^2\beta_m \frac{d^3\theta_2}{d\tau^2 d\eta} - \frac{32}{9}Ib6\alpha_m{}^2\beta_m \frac{d^3\theta_2}{d\tau^2 d\eta} - 16Q_{66}Ib4\beta_m \frac{d\theta_2}{d\eta}$$
$$+8Q_{66}Ib2\beta_m \frac{d\theta_2}{d\eta} + 2\alpha_m{}^2 \frac{d^2W}{d\tau^2} + G_{31}\alpha_m \frac{d^2U}{d\tau \mathrm{d}\zeta} + G_{32}\alpha_m \frac{d^2V}{d\tau \mathrm{d}\eta} - Q_{55}\alpha_m{}^2 \frac{d^2W}{d\zeta^2} + c_{bd}\alpha_m \frac{dW}{d\tau} \quad (19)$$
$$+8/3Ib4\alpha_m{}^3 \frac{d^3\theta_1}{d\tau^2 d\zeta} - \frac{32}{9}Ib6\alpha_m{}^4 \frac{d^4W}{d\tau^2 d\zeta^2} - Q_{66}\beta_m{}^2 \frac{d^2W}{d\eta^2} - \frac{32}{9}Ib6\alpha_m{}^3 \frac{d^3\theta_1}{d\tau^2 d\zeta}$$
$$-Q_{66}\beta_m \frac{d\theta_2}{d\eta} - Q_{55}\alpha_m \frac{d\theta_1}{d\zeta} + \frac{16}{9}Q_{21}Ib6\beta_m{}^2\alpha_m \frac{d^3\theta_1}{d\eta^2 d\zeta} - 4/3Q_{12}Ib4\beta_m{}^2\alpha_m \frac{d^3\theta_1}{d\eta^2 d\zeta}$$
$$+\frac{32}{9}Q_{44}Ib6\beta_m{}^2\alpha_m \frac{d^3\theta_1}{d\eta^2 d\zeta} - 4/3Q_{21}Ib4\beta_m{}^2\alpha_m \frac{d^3\theta_1}{d\eta^2 d\zeta} + \frac{16}{9}Q_{12}Ib6\beta_m{}^2\alpha_m \frac{d^3\theta_1}{d\eta^2 d\zeta}$$
$$-8/3Q_{44}Ib4\beta_m{}^2\alpha_m \frac{d^3\theta_1}{d\eta^2 d\zeta} + \frac{32}{9}Q_{44}Ib6\alpha_m{}^2\beta_m \frac{d^3\theta_2}{d\eta \mathrm{d}\zeta^2} - 4/3Q_{21}Ib4\alpha_m{}^2\beta_m \frac{d^3\theta_2}{d\eta \mathrm{d}\zeta^2}$$
$$-4/3Q_{12}Ib4\alpha_m{}^2\beta_m \frac{d^3\theta_2}{d\eta \mathrm{d}\zeta^2} - 8/3Q_{44}Ib4\alpha_m{}^2\beta_m \frac{d^3\theta_2}{d\eta \mathrm{d}\zeta^2} + \frac{16}{9}Q_{21}Ib6\alpha_m{}^2\beta_m \frac{d^3\theta_2}{d\eta \mathrm{d}\zeta^2}$$
$$+\frac{16}{9}Q_{12}Ib6\alpha_m{}^2\beta_m \frac{d^3\theta_2}{d\eta \mathrm{d}\zeta^2} + \frac{64}{9}Q_{44}Ib6\alpha_m{}^2\beta_m{}^2 \frac{d^4W}{d\eta^2 d\zeta^2} + \frac{32}{9}Q_{12}Ib6\alpha_m{}^2\beta_m{}^2 \frac{d^4W}{d\eta^2 d\zeta^2}$$
$$+\frac{32}{9}Q_{21}Ib6\alpha_m{}^2\beta_m{}^2 \frac{d^4W}{d\eta^2 d\zeta^2}w_0 + K_{bw}W - g_{xa}\alpha\cos^2\Omega \frac{d^2W}{d\zeta^2} - 2g_{xa}\beta\sin\Omega\cos\Omega \frac{d^2W}{d\eta d\zeta}$$
$$-g_{xb}\beta\sin^2\Omega \frac{d^2W}{d\eta^2} - g_{ya}\alpha\sin^2\Omega \frac{d^2W}{d\zeta^2} + 2g_{ya}\beta\sin\Omega\cos\Omega \frac{d^2W}{d\eta d\zeta} - g_{yb}\beta\cos^2\Omega \frac{d^2W}{d\eta^2})_{Sheet},$$

$$\delta\theta_1 = \delta\theta_{1Core} + \delta\theta_{1Sheet} = (\frac{23}{30}C_{55}\delta\theta_1 + \frac{2}{315}C_{12}\delta\beta^2\alpha\frac{d^3W}{d\eta^2 d\zeta} + \frac{4}{315}C_{44}\delta\beta^2\alpha\frac{d^3W}{d\eta^2 d\zeta} + \frac{4}{15}C_{55}\delta\alpha\frac{dW}{d\zeta}$$
$$+\frac{2}{315}C_{21}\delta\beta^2\alpha\frac{d^3W}{d\eta^2 d\zeta} - \frac{17}{630}C_{12}\delta\beta\alpha\frac{d^2\theta_2}{d\eta\zeta} - \frac{17}{630}C_{44}\delta\beta\alpha\frac{d^2\theta_2}{d\eta\zeta} + \frac{4}{315}C_{11}\delta\alpha^3\frac{d^3W}{d\zeta^3}$$
$$-\frac{17}{630}C_{21}\delta\beta\alpha\frac{d^2\theta_2}{d\eta\zeta} - \frac{17}{630}C_{44}\delta\beta^2\frac{d^2\theta_1}{d\eta^2} - \frac{17}{315}C_{11}\delta\alpha^2\frac{d^2\theta_1}{d\zeta^2} + \frac{17}{315}\delta\alpha^2\epsilon\frac{d^2\theta_1}{d\tau^2} - \frac{4}{315}\delta\alpha^3\epsilon\frac{d^3W}{d\tau^2 d\zeta})_{Core}$$
$$+(Q_{55}\theta_1 - \frac{32}{9}Q_{11}Ib6\alpha_m^3\frac{d^3W}{d\zeta^3} - 8Q_{55}Ib2\alpha_m\frac{dW}{d\zeta} + 16Q_{55}Ib4\alpha_m\frac{dW}{d\zeta} + 8/3Q_{44}Ib4\beta_m{}^2\frac{d^2\theta_1}{d\eta^2}$$
$$-\frac{16}{9}Q_{44}Ib6\beta_m{}^2\frac{d^2\theta_1}{d\eta^2} + 16/3Q_{11}Ib4\alpha_m{}^2\frac{d^2\theta_1}{d\zeta^2} - \frac{32}{9}Q_{11}Ib6\alpha_m^2\frac{d^2\theta_1}{d\zeta^2} - Q_{44}Ib2\beta_m^2\frac{d^2\theta_1}{d\eta^2} -$$
$$2Q_{11}Ib2\beta_m^2\frac{d^2\theta_1}{d\zeta^2} + 8/3Q_{11}Ib4\alpha_m^3\frac{d^3W}{d\zeta^3} + 4/3Q_{21}Ib4\beta_m^2\alpha_m\frac{d^3W}{d\eta^2 d\zeta} + 4/3Q_{12}Ib4\beta_m^2\alpha_m\frac{d^3W}{d\eta^2 d\zeta} \quad (20)$$
$$-\frac{32}{9}Q_{44}Ib6\beta_m^2\alpha_m\frac{d^3W}{d\eta^2 d\zeta} - \frac{16}{9}Q_{21}Ib6\beta_m^2\alpha_m\frac{d^3W}{d\eta^2 d\zeta} - \frac{16}{9}Q_{12}Ib6\beta_m^2\alpha_m\frac{d^3W}{d\eta^2 d\zeta}$$
$$+8/3Q_{44}Ib4\beta_m{}^2\alpha_m\frac{d^3W}{d\eta^2 d\zeta} - Q_{21}Ib2\beta_m\alpha_m\frac{d^2\theta_2}{d\eta d\zeta} + 8/3Q_{21}Ib4\beta_m\alpha_m\frac{d^2\theta_2}{d\eta d\zeta} - \frac{16}{9}Q_{12}Ib6\beta_m\alpha_m\frac{d^2\theta_2}{d\eta\zeta}$$
$$-\frac{16}{9}Q_{44}Ib6\beta_m\alpha_m\frac{d^2\theta_2}{d\eta d\zeta} - \frac{16}{9}Q_{21}Ib6\beta_m\alpha_m\frac{d^2\theta_2}{d\eta d\zeta} + 8/3Q_{44}Ib4\beta_m\alpha_m\frac{d^2\theta_2}{d\eta d\zeta} + 8/3Q_{12}Ib4\beta_m\alpha_m\frac{d^2\theta_2}{d\eta d\zeta}$$
$$-Q_{12}Ib2\beta_m\alpha_m\frac{d^2\theta_2}{d\eta d\zeta} - Q_{44}Ib2\beta_m\alpha_m\frac{d^2\theta_2}{d\eta d\zeta} + \frac{32}{9}Ib6\alpha_m{}^2\frac{d^2\theta_1}{d\tau^2} + 2Ib2\alpha_m{}^2\frac{d^2\theta_1}{d\tau^2} + \frac{32}{9}Ib6\alpha_m{}^3\frac{d^3W}{d\tau^2 d\zeta}$$
$$-8Q_{55}Ib2\theta_1 - 16/3Ib4\alpha_m{}^2\frac{d^2\theta_1}{d\tau^2} + 16Q_{55}Ib4\theta_1 - 8/3Ib4\alpha_m{}^3\frac{d^3W}{d\tau^2 d\zeta} + Q_{55}\alpha_m\frac{dW}{d\zeta})_{Sheet},$$

$$\delta\theta_2 = \delta\theta_{2Core} + \delta\theta_{2Sheet} = (\frac{4}{15}C_{66}\delta\theta_2 + \frac{2}{315}C_{12}\delta\alpha^2\beta\frac{d^3W}{d\eta\zeta^2} + \frac{2}{315}C_{21}\delta\alpha^2\beta\frac{d^3W}{d\eta\zeta^2} - \frac{17}{630}C_{12}\delta\alpha\beta\frac{d^2\theta_1}{d\eta\zeta}$$
$$+\frac{4}{315}C_{22}\delta\beta^3\frac{d^3W}{d\eta^3} - \frac{17}{630}C_{44}\delta\alpha\beta\frac{d^2\theta_1}{d\eta\zeta} + \frac{4}{315}C_{44}\delta\alpha^2\beta\frac{d^3W}{d\eta\zeta^2} - \frac{17}{630}C_{21}\delta\alpha\beta\frac{d^2\theta_1}{d\eta\zeta} + \frac{4}{15}C_{66}\delta\beta\frac{dW}{d\eta}$$
$$-\frac{17}{630}C_{44}\delta\alpha^2\frac{d^2\theta_2}{d\zeta^2} - \frac{17}{315}C_{22}\delta\beta^2\frac{d^2\theta_2}{d\eta^2} + \frac{17}{315}\delta\alpha^2\epsilon\frac{d^2\theta_2}{d\tau^2} - \frac{4}{315}\delta\alpha^3\epsilon\frac{d^3W}{d\tau^2 d\zeta})_{Core} + Q_{66}\theta_2$$
$$+Q_{66}\beta_m\frac{dW}{d\eta} + 16Q_{66}Ib4\theta_2 + 2Ib2\alpha_m^2\frac{d^2\theta_2}{d\tau^2} + 4/3Q_{12}Ib4\beta_m\alpha_m^2\frac{d^3W}{d\eta d\zeta^2} - \frac{32}{9}Q_{44}Ib6\beta_m\alpha_m^2\frac{d^3W}{d\eta d\zeta^2}$$
$$+4/3Q_{21}Ib4\beta_m\alpha_m^2\frac{d^3W}{d\eta d\zeta^2} - \frac{16}{9}Q_{12}Ib6\beta_m\alpha_m{}^2\frac{d^3W}{d\eta d\zeta^2} - \frac{16}{9}Q_{21}Ib6\beta_m\alpha_m{}^2\frac{d^3W}{d\eta d\zeta^2}$$
$$+8/3Q_{44}Ib4\beta_m\alpha_m{}^2\frac{d^3W}{d\eta d\zeta^2} - \frac{16}{9}Q_{44}Ib6\beta_m\alpha_m\frac{d^2\theta_1}{d\eta d\zeta} - \frac{16}{9}Q_{21}Ib6\beta_m\alpha_m\frac{d^2\theta_1}{d\eta d\zeta} - Q_{21}Ib2\beta_m\alpha_m\frac{d^2\theta_1}{d\eta d\zeta} \quad (21)$$
$$-Q_{12}Ib2\beta_m\alpha_m\frac{d^2\theta_1}{d\eta d\zeta} + 8/3Q_{12}I4b\beta_m\alpha_m\frac{d^2\theta_1}{d\eta d\zeta} - Q_{44}Ib2\beta_m\alpha_m\frac{d^2\theta_1}{d\eta d\zeta} + 8/3Q_{44}Ib4\beta_m\alpha_m\frac{d^2\theta_1}{d\eta d\zeta}$$
$$+8/3Q_{21}Ib4\beta_m\alpha_m\frac{d^2\theta_1}{d\eta d\zeta} - \frac{16}{9}Q_{12}Ib6\beta_m\alpha_m\frac{d^2\theta_1}{d\eta d\zeta} - 8Q_{66}Ib2\beta_m\frac{dW}{d\eta} + 16Q_{66}Ib4\beta_m\frac{dW}{d\eta}$$
$$+8/3Q_{22}Ib4\beta_m{}^3\frac{d^3W}{d\eta^3} - \frac{32}{9}Q_{22}Ib6\beta_m{}^3\frac{d^3W}{d\eta^3} - 8/3Ib4\beta_m\alpha_m{}^2\frac{d^3W}{d\tau^2 d\eta} + \frac{32}{9}Ib6\beta_m\alpha_m^2\frac{d^3W}{d\tau^2 d\eta}$$
$$-\frac{32}{9}Q_{22}Ib6\beta_m^2\frac{d^2\theta_2}{d\eta^2} - \frac{16}{9}Q_{44}Ib6\alpha_m^2\frac{d^2\theta_2}{d\zeta^2} + 8/3Q_{44}Ib4\alpha_m^2\frac{d^2\theta_2}{d\zeta^2} + 16/3Q_{22}Ib4\beta_m^2\frac{d^2\theta_2}{d\eta^2}$$
$$-2Ib2\beta_m{}^2Q_{22}\frac{d^2\theta_2}{d\eta^2} - Q_{44}Ib2\alpha_m{}^2\frac{d^2\theta_2}{d\zeta^2} + \frac{32}{9}Ib6\alpha_m{}^2\frac{d^2\theta_2}{d\tau^2} - 8Q_{66}Ib2\theta_2 - 16/3Ib4\alpha_m{}^2\frac{d^2\theta_2}{d\tau^2})_{Sheet}$$

where $Ii = \int_{h_c/2}^{(h_c/2+h_m)} z^i \, dz + \int_{-(h_c/2+h_m)}^{-h_c/2} z^i \, dz, \quad (i = 2,4,6)$.

8 SOLUTION PROCEDURE USING DIFFERENTIAL QUADRATURE METHOD (DQM)

Initially, the following equations are replaced in the equations of motion to allow for temporal and spatial discretization:

$$\begin{aligned} &U(\zeta,\eta,\tau) = U(\zeta,\eta)\ e^{\omega\tau}, \qquad V(\zeta,\eta,\tau) = V(\zeta,\eta)\ e^{\omega\tau}, \qquad W(\zeta,\eta,\tau) = W(\zeta,\eta)\ e^{\omega\tau}, \\ &\theta_1(\zeta,\eta,\tau) = \theta_1(\zeta,\eta)\ e^{\omega\tau}, \qquad \theta_2(\zeta,\eta,\tau) = \theta_2(\zeta,\eta)\ e^{\omega\tau}, \end{aligned} \tag{22}$$

where $\omega = \Omega a\sqrt{\frac{\rho_m}{E_m}}$ is the dimensionless frequency (Ω is the dimension frequency). DQM can change the differential equations into the first algebraic equations. In this regard, the partial derivatives of a function (F) are approximated by a specific variable, at discontinuous points by a set of weighting series. It's supposed that F be a function representing U, V, W, θ_1 and θ_2 with respect to variables ξ and η ($0 < \xi < 1, 0 < \eta < 1$) when $N_\xi \times N_\eta$ be the grid points along these variables with following derivative [41-42]:

$$\begin{aligned} &\frac{d^n F(\xi_i,\eta_j)}{d\xi^n} = \sum_{k=1}^{N_\xi} A_{ik}^{(n)} F(\xi_k,\eta_j) \qquad n = 1,\ldots,N_\xi - 1, \\ &\frac{d^m F(\xi_i,\eta_j)}{d\eta^m} = \sum_{l=1}^{N_\eta} B_{jl}^{(m)} F(\xi_i,\eta_l) \qquad m = 1,\ldots,N_\eta - 1, \\ &\frac{d^{n+m} F(\xi_i,\eta_j)}{d\xi^n d\eta^m} = \sum_{k=1}^{N_\xi}\sum_{l=1}^{N_\eta} A_{ik}^{(n)} B_{jl}^{(m)} F(\xi_k,\eta_l), \end{aligned} \tag{23}$$

where $A_{ik}^{(n)}$ and $B_{jl}^{(m)}$ are the weighting coefficients using Chebyshev polynomials for the positions of the grid points whose recursive formulae can be found in [41]. Applying DQM and using (23) into governing (17-21), the standard form of equation of motion $(M\ddot{X} + C\dot{X} + KX = 0)$ are obtained. Considering simply supported boundary conditions an eigenvalue problem is derived in which the eigen-values of state-space matrix $\left(\left[\text{state}-\text{space}\right] = \begin{bmatrix} [0] & [\text{I}] \\ -[\text{M}]^{-1}[\text{K}] & -[\text{M}]^{-1}[\text{C}] \end{bmatrix}\right)$ are introduced as the dimensionless frequency. It is worth to mention that M is the mass matrix, C is the damping matrix and K is the stiffness, $[\text{I}]$ and $[0]$ are the unitary and zero matrices.

9 NUMERICAL RESULTS AND DISCUSSION

In this work, free vibration of sandwich plate was analyzed when the plate is subjected to biaxial in-plane forces. The sandwich plate was contained an elastic composite core that reinforced by CNT fibers. The fibers were uniformly distributed and their material properties were obtained by the rule of mixture. Two smart face sheets surrounded the CNTRC core where the three layers vibrated as an integrated structure. A feedback loop was used to control the vibration of sandwich plate in presence of magnetic field. In order to investigate the stability of sandwich, orthotropic visco-elastic Pasternak model were also used. Then, the vibration response of sandwich plate was investigated by velocity feedback gain, aspect ratio, CFTR, thickness ratio, volume fraction of fibers,

temperature, in-plane forces, orthotropic angle and damping coefficients of elastic medium. The face sheets have been made of Terfenol-D and its properties have been listed at Table 5.

Table 5
Material properties of face sheet (Terfnol_D) and matrix (PmPV) [9,13].

Properties	E	υ	ρ	$e_{31}=e_{32}$
Terfenol-D	$30\times10^9\ Pa$	0.25	$9.25\times10^3\ kg/m^3$	$442.55N/(m.A)$
PmPV	$(3.51-0.0047T)\ GPa$	0.34	$1190\ kg/m^3$	-

At first, to ensure the correct results, linear frequency $\omega=\Omega a^2\sqrt{\frac{\rho.h}{D}}$, $D=\frac{EI}{(1-\upsilon^2)}$ for an isotropic square plate has been compared in Table 6 for three modes. A good agreement among the results of present work and other published papers [8,43-45] shows that the correct solution is used.

Table 6
Comparison of linear frequency for an isotropic square plate $(\gamma=1,\ \beta=1/300,\ \upsilon=0.3)$.

	ω_{11}	ω_{12}	ω_{13}
Leissa [43]	19.7392	49.3480	98.6960
Bardell [44]	19.7392	49.3480	98.7162
Wang et al. [45]	19.7392	49.3453	98.6268
Wang and Shen [8]	19.7362	49.3431	98.6765
Present work	19.4250	49.3392	98.0423

Fig. 2 shows the dimensionless frequency of the sandwich plate when the in-plane forces are applied in x and y direction. The volume fraction 0.17 has been selected for reinforcement of composite. In-plane forces are more effective when its intensity grows but it is necessary to limit and control according to the corresponding dimensionless group. Here all of logical data have been chosen so that the effect of the in-plane forces is clearly shown. In-plane force in y direction is related to in-plane force in x direction by χ coefficient where $N_y=\chi N_x$. Both negative and positive values of the in-plane forces have been presented in Fig. 2 while increasing χ increases the force intensity in y direction. The positive and negative values represent the compression and tension forces, respectively, since the in-plane forces are vector quantity. It's concluded from Fig. 3 that the in-plane compression forces cause to decrease the dimensionless frequency and consequently, system instability. On the other hand, the tension forces increase the frequency and system becomes more stable. It's clear from the figure that χ have opposite effect in compression and tension forces. The minus values of χ means that the sign of N_x and N_y is opposite. All curves in Fig. 2 converge to one point in Nb=0 because in this case the in-plane loading is zero, thus all results are the same.

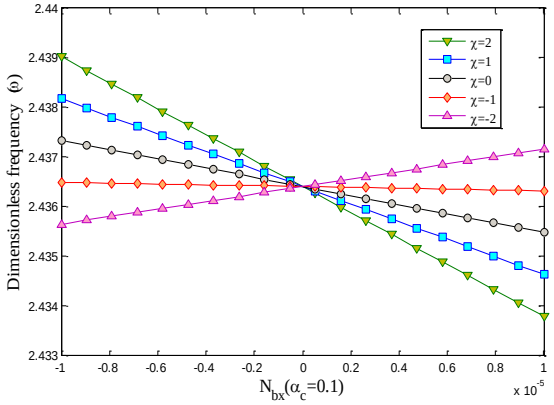

Fig.2
Variation of ω when the in-plane forces are applied in x and y directions.

Fig. 3 have been drawn to show the effect of orthotropic angle on the dimensionless frequency in different parameter of λ. As can be seen from the Fig. 3, by increasing the orthotropic angle from 0° *or* $0(radian)$ to 90° *or* $0.5\pi(radian)$, the dimensionless natural frequency decreases and Symmetrically increased from 90° *or* $\pi/2(radian)$ to 180° *or* $\pi(radian)$. This trend is the same for all values of λ. According to $g_{ya}=\frac{g_{xa}}{\lambda}$, increase of λ leads to reduce of g_{ya} and the elastic medium becomes week, so the dimensionless frequency decreases.

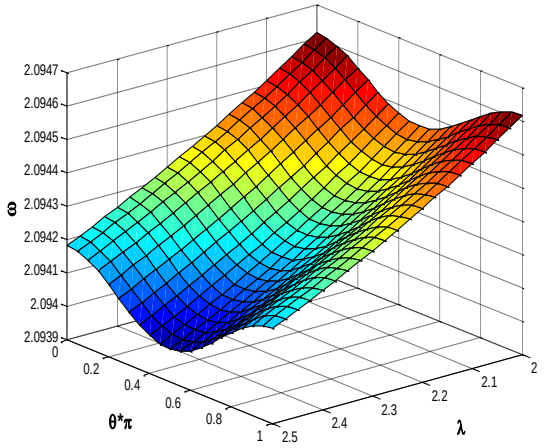

Fig.3
Effect of orthotropic angle on the dimensionless frequency for different parameter of λ.

Fig. 4 displays the effect of uniaxial in-plane force and core-to-face sheet thickness ratio on dimensionless frequency. As can be seen from the figure, increasing δ causes to decrease of dimensionless frequency of sandwich plate because the effective elastic coefficient of composite core is lower than Terfenol-D face sheets in almost all of cases. So, when the thickness of composite core increase, the stiffness of sandwich decreases and the dimensionless frequency also reduces. This result remains in presence of tension $(N_x<0)$ and comparison $(N_x>0)$ loads.

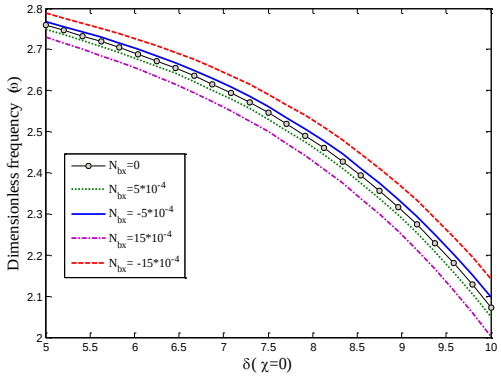

Fig.4
Effect of uniaxial in-plane forces on ω for different sandwich core-to-face sheet thickness ratios.

Fig. 5 shows the effect of volume fraction of CNT as a fiber of composite core on dimensionless frequency. There are three cases for volume fraction of CNTs in which the material properties have been compared with MD results according to the rule of mixture. CNT efficiency parameter and other elastic properties have been reported in Tables 1-3. Fig. 5 clearly shows the effect of fibers on strength of the core where increasing volume fraction from $V_{CNT}=0.11 to\ 0.17$ leads to increase the dimensionless frequency significantly.

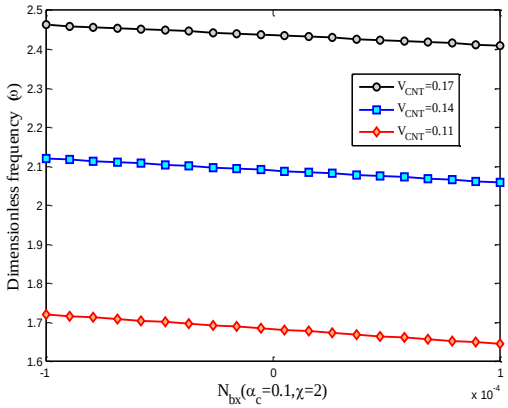

Fig.5
Effect of volume fraction of composite fibers on dimensionless frequency of sandwich plate.

Fig. 6 shows the effect of elastic medium on dimensionless frequency of sandwich plate. It's evident when the normal and shear modulus of elastic medium increase, the stiffness increase and it's make a more stable system but these increase is practically limited. Damping is an influence within or upon an oscillatory system that has the effect of reducing, restricting or preventing its oscillations. In physical systems, damping is produced by processes that dissipate the energy stored in the oscillation for example viscous drag in mechanical systems.

Linear damping is a mathematically useful attenuation. Linear damping is manifested when a potentially oscillatory variable is directly reduced by the instantaneous rate of change, velocity, or time derivative [46]. Fig. 6 also illustrates the linear damping effect on dimensionless frequency of sandwich plate. As can be seen from the figure and according to above explanation, damping coefficient leads to decrease of dimensionless frequency.

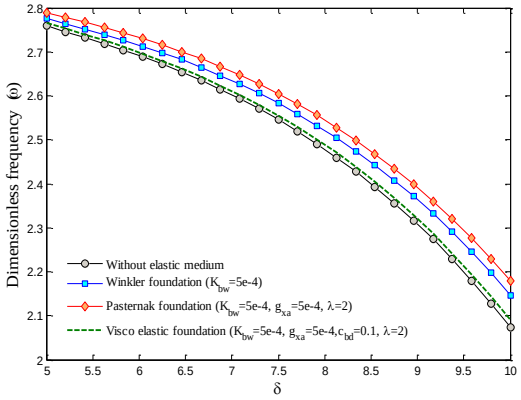

Fig.6
Effect of elastic medium on dimensionless frequency of sandwich plate.

Since the material properties of CNT fibers have been reported for different temperature, Fig. 7 shows the vibrational response of sandwich plate in these temperatures. It's clear from the figure that increasing the temperature lead to decrease the dimensionless frequency because the elastic properties of CNT such as Young's and shear modulus change so that the structure becomes softer.

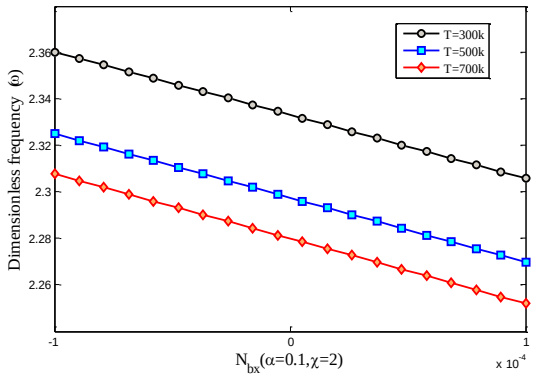

Fig.7
Effect of temperature change on dimensionless frequency of sandwich plate.

It should be noted when the MsMs is exposed to magnetic field, they deform due to reciprocal nature. By changing in velocity feedback gain parameter K_{vfc} can be controlled the MsP frequency. As it is shown in Fig. 8, increasing velocity feedback gain leads to decrease the frequency of MsP, significantly. Magnetic field is varied using a control feedback system in order to vibrational behavior analysis of CNTR composite- magnetostrictive faced sandwich plate. Fig. 8 shows the effect of appropriate velocity feedback gain on the dimensionless frequency. It is worth mentioning that in the large values of core-to-face sheet thickness ratio, the effect of the control feedback system is weak and the peaks of curve fall to the bottom where the positive and negative magnetization has been considered.

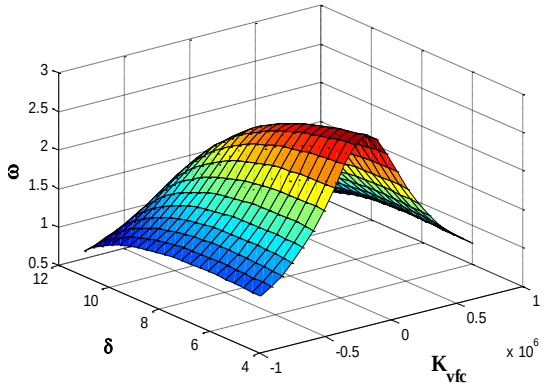

Fig.8
Effect of velocity feedback gain on ω versus core-to-face sheet thickness ratios.

Fig. 9 is a three dimensional plot of variation of dimensionless frequency for four cases of harmonic in-plane loads as follows:

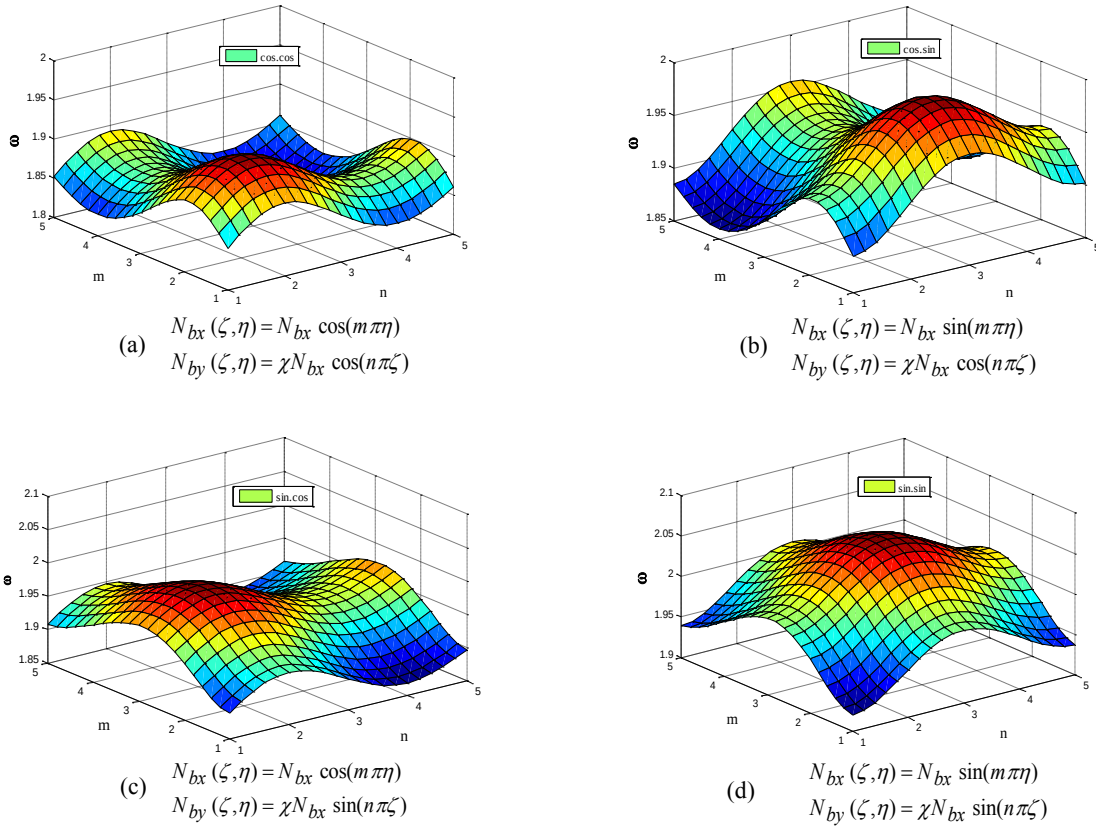

(a) $N_{bx}(\zeta,\eta) = N_{bx}\cos(m\pi\eta)$, $N_{by}(\zeta,\eta) = \chi N_{bx}\cos(n\pi\zeta)$

(b) $N_{bx}(\zeta,\eta) = N_{bx}\sin(m\pi\eta)$, $N_{by}(\zeta,\eta) = \chi N_{bx}\cos(n\pi\zeta)$

(c) $N_{bx}(\zeta,\eta) = N_{bx}\cos(m\pi\eta)$, $N_{by}(\zeta,\eta) = \chi N_{bx}\sin(n\pi\zeta)$

(d) $N_{bx}(\zeta,\eta) = N_{bx}\sin(m\pi\eta)$, $N_{by}(\zeta,\eta) = \chi N_{bx}\sin(n\pi\zeta)$

Fig.9
Effect of harmonic in-plane forces on dimensionless frequency of sandwich.

The effect of the dimensionless image and real natural frequency versus the follower force for various values of the elastic foundation parameters has been shown in Fig. 10(a) and (b), respectively. It is seen that with considering two parameters elastic foundation, the stability region increases and the structure becomes more stable.

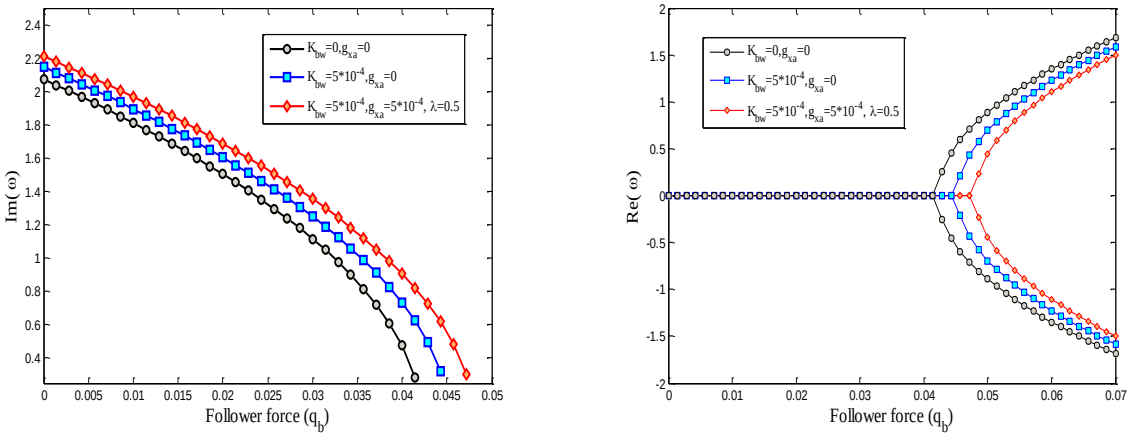

(a) (b)

Fig.10
The effect of the dimensionless image (a) and real (b) natural frequency versus the follower force for various values of the elastic foundation parameters.

10 CONCLUSIONS

Free vibration of sandwich plate with composite core and magnetostrictive face sheet is a novel topic that has been studied in this research for the first time. To consider the magnetization effect of face sheet, a control feedback system was used and velocity feedback gain as controlling parameter introduced. Orthotropic visco-Pasternak foundation was developed to evaluate the orthotropic angle, damping coefficient, Young's and shear modulus. Sandwich plate undergoes the in-plane forces that can be distributed on each face sheets and core individually. Reddy's plate as a third order shear deformation plat theory was used to derive the equations of motion. Two-dimensional DQM was utilized to solve the equations of motion and following results were concluded:

- ❖ Orthotropic vico-Pasternak foundation plays an important role on stability of sandwich plate so that:
  - ✓ Normal (k_{bw}) and shear modulus (g_x) significantly increase the dimensionless frequency of sandwich plate.
  - ✓ Damping coefficient lead to decrease of dimensionless frequency especially in lower α so that in large value of α the curves converge to the same value.
  - ✓ Changes in the Young's and shear modulus of the orthotropic elastic foundation, the intensity and tendency of the orthotropy changes, but generally the change is slight.
  - ✓ Unlike tension forces, In-plane compression forces lead to decrease the stability of the system.
- ❖ Compression in-plane forces decrease the dimensionless frequency of sandwich plate and cause the instability of system but tension in-plane force increase the frequency and leads to more stability.
- ❖ Both face sheets can be utilized to vibration suppression of sandwich plate using control feedback system where velocity feedback gain as a control parameter reduces the frequency of sandwich plate. Also the effect of velocity feedback gain continues so far the frequency tends to constant value for all of parameters but it's possible for very precise controller.

REFERENCES

[1] Reddy J.N., 2003, *Mechanics of Laminated Composite Plates and Shells: Theory and Analysis*, CRC press, Boca Raton.

[2] Mohammadimehr M., Rousta Navi B., Ghorbanpour Arani A., 2017, Dynamic stability of modified strain gradient theory sinusoidal viscoelastic piezoelectric polymeric functionally graded single-walled carbon nanotubes reinforced

nanocomposite plate considering surface stress and agglomeration effects under hydro-thermo-electro-magneto-mechanical loadings, *Mechanics of Advanced Materials and Structures* **24**(16): 1325-1342.

[3] Mohammadimehr M., Mohammadimehr M.A., Dashti P., 2016, Size-dependent effect on biaxial and shear nonlinear buckling analysis of nonlocal isotropic and orthotropic micro-plate based on surface stress and modified couple stress theories using differential quadrature method, *Applied Mathematics and Mechanics* **37**(4): 529-554.

[4] AkhavanAlavi S.M., Mohammadimehr M., Edjtahed S.H., 2019, Active control of micro Reddy beam integrated with functionally graded nanocomposite sensor and actuator based on linear quadratic regulator method, *European Journal of Mechanics A/Solids* **74**: 449-461.

[5] Ghorbanpour Arani A., Rousta Navi B., Mohammadimehr M., 2016, Surface stress and agglomeration effects on nonlocal biaxial buckling polymeric nanocomposite plate reinforced by CNT using various approaches, *Advanced Composite Materials* **25**(5): 423-441.

[6] Alipour M.M., Shariyat M., 2020, Using orthotropic viscoelastic representative elements for C1-continuous zigzag dynamic response assessment of sandwich FG circular plates with unevenly damaged adhesive layers, *Mechanics Based Design of Structures and Machines* **49**(3): 355-380.

[7] Panda S., Ray M.C., 2009, Active control of geometrically nonlinear vibrations of functionally graded laminated composite plates using piezoelectric fiber reinforced composites, *Journal of Sound and Vibration* **325**(1-2): 186-205.

[8] Wang Z.X., Shen H.S., 2012, Nonlinear vibration and bending of sandwich plates with nanotube-reinforced composite face sheets, *Composites Part B: Engineering* **43**(2): 411-421.

[9] Lei Z.X., Liew K.M., Yu J.L., 2013, Free vibration analysis of functionally graded carbon nanotube-reinforced composite plates using the element-free kp-Ritz method in thermal environment, *Composite Structures* **106**: 128-138.

[10] Natarajan S., Haboussi M., Manickam G., 2014, Application of higher-order structural theory to bending and free vibration analysis of sandwich plates with CNT reinforced composite facesheets, *Composite Structures* **113**: 197-207.

[11] Malekzadeh K., Khalili S.M.R., Abbaspour P., 2010, Vibration of non-ideal simply supported laminated plate on an elastic foundation subjected to in-plane stresses, *Composite Structures* **92**: 1478-1484.

[12] Lee S.J., Reddy J.N., Rostam-Abadi F., 2004, Transient analysis of laminate embedded smart-material layers, *Finite Elements in Analysis and Design* **40**(5-6): 463-483.

[13] Hong C.C., 2010, Transient responses of magnetostrictive plates by using the GDQ method, *European Journal of Mechanics A/Solids* **29**(6): 1015-1021.

[14] Sahoo R., Singh B.N., 2013, A new shear deformation theory for the static analysis of laminated composite and sandwich plates, *International Journal of Mechanical Sciences* **75**: 324-336.

[15] Ghorbanpour Arani A., Khoddami Maraghi Z., 2016, A feedback control system for vibration of magnetostrictive plate subjected to follower force using sinusoidal shear deformation theory, *Ain Shams Engineering Journal* **7**(1): 361-369.

[16] Zhang L.W., Lei Z.X., Liew K.M., 2015, Vibration characteristic of moderately thick functionally graded carbon nanotube reinforced composite skew plates, *Composite Structures* **122**: 172-183.

[17] Kiani Y., 2016, Free vibration of functionally graded carbon nanotube reinforced composite plates integrated with piezoelectric layers, *Computers & Mathematics with Applications* **72**(9): 2433-2449.

[18] Selim B.A., Zhang L.W., Liew K.M., 2017, Active vibration control of CNT reinforced composite plates with piezoelectric layers based on Reddy's higher-order shear deformation theory, *Composite Structures* **163**: 350-364.

[19] Lei Z.X., Zhang L.W., Liew K.M., 2016, Vibration of FG-CNT reinforced composite thick quadrilateral plates resting on Pasternak foundations, *Engineering Analysis with Boundary Elements* **64**: 1-11.

[20] Duc N.D., Lee J., Nguyen-Thoi T., Thang P.T., 2017, Static response and free vibration of functionally graded carbon nanotube-reinforced composite rectangular plates resting on Winkler-Pasternak elastic foundations, *Aerospace Science and Technology* **68**: 391-402.

[21] Keleshteri M.M., Asadi H., Wang Q., 2017, Large amplitude vibration of FG-CNT reinforced composite annular plates with integrated piezoelectric layers on elastic foundation, *Thin-Walled Structures* **120**: 203-214.

[22] Mohammadimehr M., Salemi M., Rousta Navi B., 2016, Bending, buckling, and free vibration analysis of MSGT microcomposite Reddy plate reinforced by FG-SWCNTs with temperature- dependent material properties under hydro-thermo-mechanical loadings using DQM, *Composite Structures* **138**: 361-380.

[23] Ansari R., Torabi J., Hasrati E., 2018, Axisymmetric nonlinear vibration analysis of sandwich annular plates with FGCNTRC face sheets based on the higher-order shear deformation plate theory, *Aerospace Science and Technology* **77**: 306-319.

[24] Shen H.S., Wang H., Yang D.Q., 2017, Vibration of thermally postbuckled sandwich plates with nanotube-reinforced composite face sheets resting on elastic foundations, *International Journal of Mechanical Sciences* **124-125**: 253-262.

[25] Fazzolari F.A., 2018, Thermoelastic Vibration and Stability of Temperature-Dependent Carbon Nanotube-Reinforced Composite Plates, *Composite Structures* **196**: 199-214.

[26] Parida S., Mohanty S.C., 2019, Nonlinear free vibration analysis of functionally graded plate resting on elastic foundation in thermal environment using higher-order shear deformation theory, *Scientia Iranica B* **26**(2): 815-833.

[27] Sahoo S.S., Hirwani C.K., Panda S.K., Sen D., 2018, Numerical analysis of vibration and transient behaviour of laminated composite curved shallow shell structure: An experimental validation, *Scientia Iranica B* **25**(4): 2218-2232.

[28] Shen H.S., 2009, Nonlinear bending of functionally graded carbon nanotube reinforced composite plates in thermal environments, *Composite Structures* **91**: 9-19.

[29] Han Y., Elliott J., 2007, Molecular dynamics simulations of the elastic properties of polymer/carbon nanotube composites, *Computational Materials Science* **39**(2): 315-323.
[30] Griebel M., Hamaekers J., 2004, Molecular dynamics simulations of the elastic moduli of polymer–carbon nanotube composites, *Computer Methods in Applied Mechanics and Engineering* **193**(17-20): 1773-1788.
[31] Sawi A.M.K., Farag M.M., 2007, Carbon nanotube reinforced composites: potential and current challenges, *Materials and Design* **28**(9): 2394-401.
[32] Fidelus J.D., Wiesel E., Gojny F.H., Schulte K., Wagner H.D., 2005, Thermo- mechanical properties of randomly oriented carbon/epoxy nanocomposites, *Composites Part A* **36**(11): 1555-1561.
[33] Hong C.C., 2009, Transient responses of magnetostrictive plates without shear effects, *International Journal of Engineering Science* **47**(3): 355-362.
[34] Krishna M., Anjanappa M., Wu Y.F., 1997, The use of magnetostrictive particle actuators for vibration attenuation of flexible beams, *Journal of Sound and Vibration* **206**(2): 133-149.
[35] Daneshmehr A., Rajabpoor A., Pourdavood M., 2014, Stability of size dependent functionally graded nano-plate based on nonlocal elasticity and higher order plate theories and different boundary conditions, *International Journal of Engineering Science* **82**: 84-100.
[36] Wang C.M., Reddy J.N., Lee K.H., 2000, *Shear Deformable Beams and Plates: Relationships with Classical Solutions*, Elsevier Science Ltd, UK.
[37] Reddy J.N., 2017, *Energy Principles and Variational Methods in Applied Mechanics*, John Wiley and Sons Publishers, Texas.
[38] Ghorbanpour Arani A., Vossough H., Kolahchi R., Barzoki A.M., 2012, Electro-thermo nonlocal nonlinear vibration in an embedded polymeric piezoelectric micro plate reinforced by DWBNNTs using DQM, *Journal of Mechanical Science and Technology* **26**(10): 3047-3057.
[39] Kutlu A., Omurtag M.H., 2012, Large deflection bending analysis of elliptic plates on orthotropic elastic foundation with mixed finite element method, *International Journal of Mechanical Sciences* **66**(1): 64-74.
[40] An C., Su J., 2014, Dynamic analysis of axially moving orthotropic plates: Integral transform solution, *Applied Mathematics and Computation* **228**: 489-507.
[41] Shu C., 2000, *Differential Quadrature and its Application in Engineering*, Springer Publishers Singapore.
[42] Mohammadimehr M., Shahedi S., Rousta Navi B., 2017, Nonlinear vibration analysis of FG-CNTRC sandwich Timoshenko beam based on modified couple stress theory subjected to longitudinal magnetic field using generalized differential quadrature method, *Proceedings of the Institution of Mechanical Engineers, Part C: Journal of Mechanical Engineering Science* **231**(20): 3866-3885.
[43] Leissa A.W., 1973, The free vibration of rectangular plates, *Journal of Sound and Vibration* **31**(3): 257-293.
[44] Bardell N.S., 1989, The application of symbolic computing to the hierarchical finite element method, *International Journal for Numerical Methods in Engineering* **28**(5): 1181-1204.
[45] Wang X., Wang Y., Chen R., 1998, Static and free vibrational analysis of rectangular plates by the differential quadrature element method, *Communications In Numerical Methods In Engineering* **14**: 1133-1141.
[46] Komkov V., 1972, *Optimal Control Theory for the Damping of Vibrations of Simple Elastic Systems*, Springer-Verlag, Berlin-New York.